ISSN 1547-4771, Physics of Particles and Nuclei Letters, 2020, Vol. 17, No. 4, pp. 463–467. © Pleiades Publishing, Ltd., 2020.
Russian Text © The Author(s), 2020, published in Pis'ma v Zhurnal Fizika Elementarnykh Chastits i Atomnogo Yadra, 2020.

PHYSICS AND TECHNIQUE OF ACCELERATORS

Electromagnetic Modeling of NICA Collider Structure Elements

P. R. Zenkevich[a, b, *] and A. A. Kolomiets[a, b]

[a] *National Research Centre Kurchatov Institute, Moscow, 123098 Russia*
[b] *Institute for Theoretical and Experimental Physics, Russian Academy of Sciences, Moscow, 117218 Russia*
**e-mail: zenkevich@itep.ru*

Received October 17, 2019; revised December 16, 2019; accepted February 28, 2020

Abstract—The coupling impedances of individual elements of the NICA collider are simulated in order to determine, at an early stage of design, the possible limitations of the beam intensity, reveal structural elements that can be the main sources of impedances, and formulate proposals for optimizing the geometry of structural elements in order to reduce the collective effects on the beam dynamics. The simulation is conducted using the CST Studio Suite commercial software [1]. The simulation results for each structural element are stored in the form of wake potentials, which can be directly used in the HEADTAIL code simulating beam dynamics. The coupling impedances are calculated from wake potentials using the Fourier transform.

DOI: 10.1134/S1547477120040512

INTRODUCTION

The interaction between the beam particles and the accelerator structural elements surrounding the beam is one of the main factors that impose limitations on the attainable parameters of the accelerator facility. When designing a new facility, the analysis of the interaction of the beam with the designed accelerator units is a necessary condition for achieving the specified parameters.

The interaction effect is characterized by the wake fields generated by particles moving in the wavefront of the bunch and which affect the motion of particles following them and the impedances representing the wake fields in the frequency domain.

Impedances are responsible for the shift of the beam oscillation frequencies; the excitation of several types of coherent instabilities; an increase in the beam emittance; and, consequently, particle loss. To estimate the frequency shift and the instability threshold, it is necessary to determine the total impedance of the accelerator facility [2]. The impedances of individual units can be determined from the results of theoretical analysis, by measuring the beam parameters in existing facilities, bench measurements, and computer simulation. Obviously, at the design stage, computer simulation is the most reliable way to determine the contribution of each individual structural element to the total impedance of the accelerator facility [3, 4].

The schematic of the basic elements of the NICA collider structure is shown in Fig. 1 [5]. The ring has the shape of a race track with two arches and two long straight sections. The vacuum chamber of the arch is formed by rectilinear segments consisting of chambers of dipole magnets with an elliptical cross section and cylindrical chambers of quadrupole magnets having sections with different diameters. Individual sections of the chambers in the arch are interconnected by bellows. The large number of inhomogeneities of the geometry and bellows make the arches a source of significant impedances of the collider.

A variety of devices located in the rectilinear sections—cavities of high-frequency system, stochastic cooling pickups, electronic cooling section, detector chambers, beam input and output devices, and collimators—are also sources of impedance, and the contribution of each device to the total impedance of the facility should be determined at the design stage.

1. CST STUDIO

In this work, we used a CST Studio program to simulate the wake potentials and calculate the corresponding impedances in individual units of the NICA collider structure. The program has a special Wakefield Solver unit for electromagnetic calculations that simulates the generation of the wake potential in the model under consideration during the passage of a generating bunch of particles. In this unit the Maxwell's equations in the time domain are solved. The standard calculation result of the program is the wake potentials created by a bunch of particles with a Gaussian distribution of particle density along the bunch. The simulation of the wake field in the Wakefield Solver of the CST STUDIO Suite is illustrated by Fig. 2. It shows the simplest model that comprises a small inhomogeneity of the cylindrical vacuum chamber, the field of the generating bunch, and the field in the analyzed element.

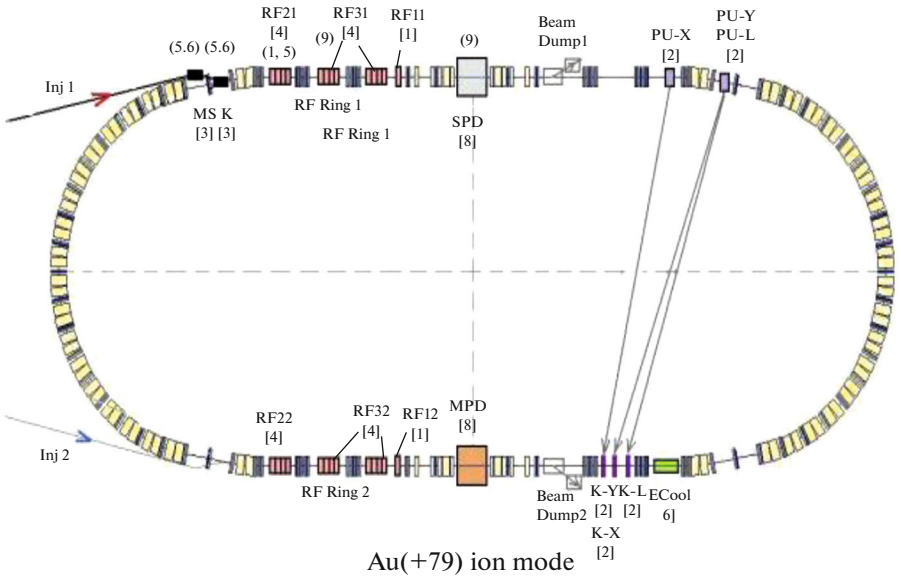

Fig. 1. Schematic of the collider ring.

In the Wakefield Solver, the wake potential (including longitudinal and transverse components) is calculated using the formula

$$\vec{W}(x_1, y_1, x_2, y_2, z) = \frac{1}{q_1 q_0} \int_0^L dz \left[\vec{E}(x_1, y_1, x_2, y_2, z, t) + \vec{v} \times \vec{B}(x_1, y_1, x_2, y_2, z, t) \right]_{t=(z+s)/c}, \quad (1)$$

where q_0 is the total charge of the bunch generating a field in the analyzed element of length L; q_1 is the test charge following the bunch at a distance s; x_1, y_1 is the transverse displacement of the bunch trajectory from the axis of the element; and x_2, y_2 is the transverse displacement of the trajectory of the test charge.

A longitudinal wake potential is usually understood as a component of potential (1) formed only by the longitudinal electric field, provided that the bunch and test charge move along the axis of the analyzed element,

$$W_{\parallel}(z) = W_{\parallel}(0,0,0,0,z).$$

In an element with axial or mirror symmetry, a bunch moving along the axis does not create transverse forces acting on the test charge, which also moves along the axis. In this case, to calculate the transverse wake potential, it is necessary to specify the displacement from the axis of the bunch or test charge. The first approximation for the expansion of the transverse components of the potential in powers of the transverse displacement has the following form [6]:

$$\begin{aligned} W_x(z) &= W_x(0,0,0,0,z) \\ &+ \nabla_x W_x(0,0,x_1,y_1,z)x_1 + \nabla_x W_x(x_0,0,0,0,z)x_0, \\ W_y(z) &= W_x(0,0,0,0,z) \\ &+ \nabla_y W_y(0,0,0,y_1,z)y_1 + \nabla_y W_y(0,y_0,0,0,z)y_0. \end{aligned} \quad (2)$$

On the right-hand side of expressions (2), the first term is the constant component on the axis of the analyzed element. For elements with axial or mirror symmetry, this term is equal to zero. The second term of the expression is usually called dipolar or driving and is denoted below as $W_{x,y}^{\mathrm{dip}}$. The third term is called quadrupolar or detuning and will be denoted as $W_{x,y}^{\mathrm{quad}}$.

Thus, to obtain the longitudinal potential, it is necessary to carry out a simulation for the case in which the bunch trajectory and the integration path coincide with the geometric axis of the analyzed element and, to obtain the components $W_{x,y}^{\mathrm{dip}}$ and $W_{x,y}^{\mathrm{quad}}$, the simulation should be performed by shifting the bunch trajectory and/or the integration path as is shown in Fig. 3 [7]. The displacement should be chosen so that,

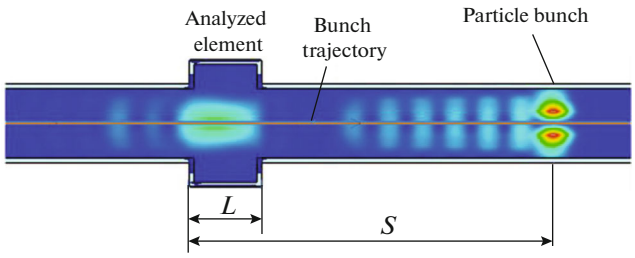

Fig. 2.

on the one hand, the linearity of the decomposition is preserved, and on the other hand, the components of the transverse impedance are defined sufficiently well.

The potentials obtained as a result of the modeling allow us to determine the corresponding impedances using the following relationships:

$$Z_{\parallel}(\omega) = -\frac{\int_{-\infty}^{\infty} W_{\parallel}(s)e^{-i\omega s}ds}{\int_{-\infty}^{\infty} \lambda(s)e^{-i\omega s}ds}, \quad (3)$$

$$Z_{\perp}(\omega) = i\frac{\int_{-\infty}^{\infty} W_{\perp}(s)e^{-i\omega s}ds}{\int_{-\infty}^{\infty} \lambda(s)e^{-i\omega s}ds}. \quad (4)$$

For each analyzed element of the collider structure, the corresponding database obtained the following data:

the longitudinal potential w_z;

the constant, dipole, and quadrupole components of the transverse potential in the X plane: $w_{x0}, w_x^{\mathrm{dip}}$, and w_x^{quad};

the constant, dipole, and quadrupole components of the transverse potential in the Y plane: $w_{y0}, w_y^{\mathrm{dip}}$, and w_y^{quad}.

The corresponding impedances were also stored:

$$Z_{\parallel},$$
$$Z_{x0}, Z_x^{\mathrm{dip}}, Z_x^{\mathrm{quad}},$$
$$Z_{y0}, Z_y^{\mathrm{dip}}, Z_y^{\mathrm{quad}}.$$

These data are sufficient both for numerical simulation of the beam motion in the collider using the HEADTAIL code and for analytical estimates of its parameters.

2. RESULTS OF SIMULATION OF THE COLLIDER CHAMBER ELEMENTS

Below are the results of the simulation of the coupling impedances obtained to March 2019. The list of the analyzed collider structure elements is given in Table 1.

Figures 4 and 5 show the total longitudinal and transverse impedances of the ring, obtained by summing the impedances of individual elements except for the RF stations. The summation of the transverse impedances was carried out according to the formula

$$Z_{\perp}(f) = \sum_{i=1}^{N} \frac{\langle \beta_{\perp}^{i} \rangle}{\langle \beta_{\perp}^{\mathrm{ring}} \rangle} Z_{\perp}^{i}(f),$$

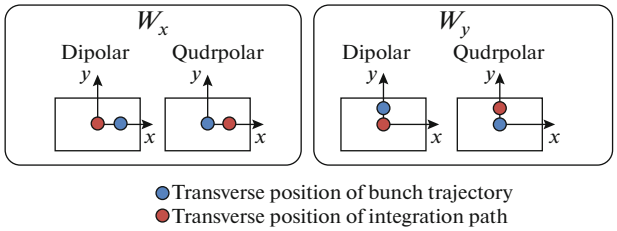

Fig. 3. Specifying the position of the bunch trajectory and the integration path for calculating transverse wake potentials.

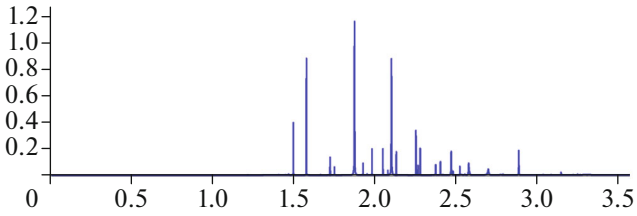

Fig. 4. Longitudinal impedance of the ring.

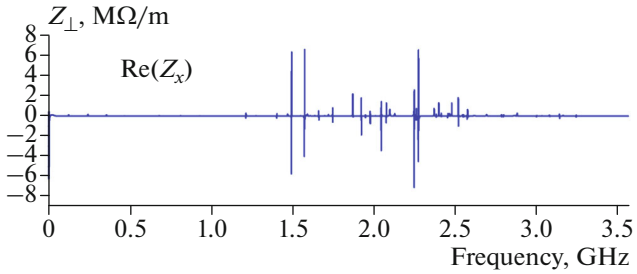

Fig. 5. Transverse impedance of ring, Z_x.

where $\langle \beta_{\perp}^{\mathrm{arch}} \rangle$ is the mean beta function of the arch, $\langle \beta_{\perp}^{\mathrm{ring}} \rangle$ is the mean beta function of the ring, and $Z_{\perp}^{i}(f)$ is the transverse impedance of the element of the arch number i [8].

As can be seen from the above figures, the impedance of the ring is clearly divided into low-frequency (below 100 MHz) and high-frequency parts. The effective impedance for the nominal collider bunch duration is determined only by the impedance at low frequency. Figures 6 and 7 show the longitudinal and transverse impedances in the low-frequency range. The longitudinal impedance in this range is negligibly small. The transverse impedance is mainly determined by the parameters of the vacuum chamber. Resonance values of the high-frequency impedance influence the microwave effects inside the beam.

Analysis has shown that all these inhomogeneities arise due to two chamber elements in the arches: (1) unshielded bellows and (2) a jump in the chamber

Table 1

	Structure elements	Amount
Arches	Dipole Magnet Chamber	80
	Quadrupole Magnet Chamber	40
	Bellow	120
	Pickup X	20
	Pickup Y	20
RF	RF station 1	1
	RF station 2	4
	RF station 3	8
Rectilinear sections	MPD	1
	Kicker SSC	?
	Pickup ECS	8
	Electron Beam Injection Chamber	2
	Collimator	4
	Kicker	1

Table 2. List of the most dangerous transverse resonances and their characteristics

Resonance no.	1	2	3	4	5	6	7	8	9	10
Frequency, GHz	0.584	0.825	1.490	1.578	1.865	2.109	2.248	2.347	2.381	2.68
$Z_\perp$, MΩ/m	2.781	1.576	3.76	6.921	30.89	10.18	141.3	16.18	26.63	8.24
Q factor	6	55	261	250	103	53	340	123	13.1	158

diameter near the quadrupole lenses. After eliminating these irregularities, the resonances practically disappear.

Figures 6 and 7 shows the impedances at low frequencies. These impedances are important for calculating the effective impedance, which determines the stability of the oscillation of the bunches.

It should be noted that the main contribution to the high-frequency part of the total impedances is made by the elements of the arches. This is due to the presence of a large number of inhomogeneities in these elements and their significant number.

To determine the impedances of the RF stations, the corresponding cavities were simulated using the Eigenmode Solver of the CST Studio Suite. Of all the resonances obtained in this way, only those that were excited by the beam as a result of using the Wakefield Solver were selected. The data of the resonance of the cavities of each RF station are given in Tables 4–6.

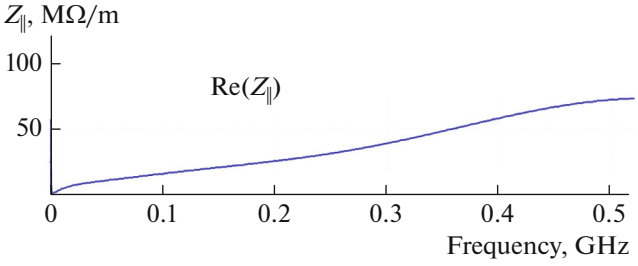

Fig. 6. Longitudinal impedance of the ring at frequencies below 500 MHz.

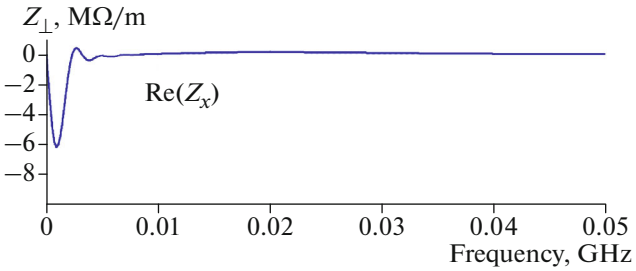

Fig. 7. Transverse impedance at frequencies below 50 MHz.

Table 3. List of the most dangerous longitudinal resonances and their characteristics

Resonance no.	1	2	3	4	5	6	7	8	9	10	12
Frequency, GHz	1.50	1.58	1.68	1.87	1.98	2.09	2.25	2.38	2.46	2.68	2.90
$Z_{\|\|}$, $\Omega \times 10^5$	1.87	4.28	1.52	8.78	1.42	7.13	3.08	1.58	2.5	51	0.24
Q factor	245	272	108	106	254	119	351	140	129	158	50

Table 4. Resonance parameters of the RF-1 station

Resonance frequency f_r, MHz	R_s, Ω	Q
118	983	339
273	2212	1334
466	955	1627
1411	38130	3324
1723	11780	3596
2180	1.152E + 06	14373

Table 5. Resonance parameters of the RF-2 station

Resonance frequency f_r, MHz	R_s, Ω	Q
452	4.9×10^3	1674
1177.6	6.74×10^3	1857
1897.9	19.8×10^3	3500

CONCLUSIONS

The main result of the simulation of the coupling impedances of the devices forming the collider's vacuum chamber is a preliminary estimation of its total impedance and contribution to the total budget of each device considered. This has served as a basis for refining the design of some devices. The simulation will continue along with making the required corrective changes in the design.

Table 6. Resonance parameters of the RF-3 station

Resonance frequency f_r, MHz	R_s, Ω	Q
30.5	9.7×10^5	8.7×10^3
595	2.3×10^4	9.7×10^3
905	$6.4\cdot \times 10^3$	2.3×10^4
1061.2	2.8×10^4	2.2×10^4
1668	3.1×10^4	1.3×10^4
2026	3.1×10^4	9.1×10^3

REFERENCES

1. CST Particle Studio. http://www.cst.com/Content/Products/PS/Overview.aspx.
2. E. Metral et al., "Beam instabilities in hadron synchrotrons," IEEE Trans. Nucl. Sci. **63**, 1001 (2016).
3. N. Biancacci, B. Salvant, and C. Zannini, "Building the impedance model of a real machine," Int. Commit. Future Accel., Beam Dyn. Newslett., No. 69, 97.
4. N. Biancacci et al., http://impedance.web.cern.ch/impedance/.
5. *Technical Design of the NICA Accelerator Complex* (Dubna, 2015) [in Russian].
6. N. Mounet, "The LHC transverse coupled bunch instability," PhD Thesis No. 5305 (Ecole Polytech. Fed. de Lausanne, Lausanne, 2012).
7. C. Zannini, "Electromagnetic simulation of CERN accelerator components and experimental applications," PhD thesis, CERN-THESIS-2013-076 (CERN, Geneva, Switzerland, 2013).
8. C. Zannini, K. Li, and G. Rumolo, "Effects of an asymmetric chamber on the beam coupling impedance," in *Proceedings of International Particle Accelerator Conference IPAC'2012, New Orleans, Louisiana, USA,* WEPPR073.

Translated by E. Chernokozhin